Interaction and Multiscale Mechanics, Vol. 5, No. 2 (2012) 157-168
DOI: http://dx.doi.org/10.12989/imm.2012.5.2.157

The dilatancy and numerical simulation of failure behavior of granular materials based on Cosserat model

Xihua Chu*, Cun Yu and Yuanjie Xu

Department of engineering mechanics, Wuhan University, Wuhan 430072, P.R. China

(Received July 15, 2011, Revised April 28, 2012, Accepted May 17, 2012)

Abstract. The dilatancy of granular materials has significant influence on its mechanical behaviors. The dilation angle is taken as a constant in conventional associated or non-associated flow rules based on Drucker-Prager yields theory. However, various experimental results show the dilatancy changes during progressive failure of granular materials. A non-associated flow rule with evolution of dilation angle is adopted in this study, and Cosserat continuum theory is used to describe the behaviors of granular materials for considering to some extent the its internal structure. Numerical examples focus on the bearing capacity and localization of granular materials, and results illustrate the capability and performance of the presented model in modeling the effect on failure behavior of granular materials.

Keywords: granular materials; Cosserat continuum model; dilation angle; bearing capacity; strain localization.

1. Introduction

Granular materials such as soil and sand are collections of discrete macroscopic solid particles. These materials have rather distinctive physical and engineering properties such as the frictional strength and dilatancy. The strength and dilatancy of granular soils have received a great deal of attention, and some agreements about the topic have been reached (Rowe 1962, Bolton 1986, Houlsby 1991, Wan and Guo 1999, Massoudi and Mehrabadi 2001, Guo and Su 2007, Alsaleh *et al*. 2009, Aristoff and Radin 2011). The dilatancy arises from the slipping or rolling between discrete particles when granular assemblies bear loading from a microscopic view. Generally, soft soils and loose sands show shearing contraction while overconsolidated clays and dense sands show shearing dilation.

The stress-dilatancy equation based on energy principles is presented by Rowe (1962), which is commonly used as a flow rule. The friction and dilation angle were assumed to be constant in the orginal Rowe's version. However, many experiments show the dilatancy changes during deformation. Studies imply that changes of dilatancy may be related to factors such as stress level, void ratio and particle crushing. Therefore, some modified stress-dilatancy equations are suggested (Wan and Guo 1999, Ueng and Chen 2000, Desimone and Tamagnini 2005, Zhang and Salgado 2010). Bolton (1986) suggested that the friction angle is the sum of the critical friction angle and

* Corresponding author, Associate professor, E-mail: Chuxh@whu.edu.cn

the dilation angle, and the dilation angle is the function of the mean effective pressure and the relative density, and the dilatancy will vanish when critical state reach. Houlsby (1991) used Wroth's critical state line function combing Bolton's empirical fit to give a flow rule. Many efforts have been devoted to understand the dilatancy of granular materials, however, as stated in the Houlsby report (1991), "the link between friction and dilatancy is well established, but quantitative expressions for the dependence of dilation on density and pressure are less known", let alone account the change of dilatancy in analysis of engineering problem.

The aim of this paper is to investigate the effect of dilatancy on the bearing capacity and strain localization of granular materials. There are some similar investigations, for example, Zienciewicz examined the effects of dilatancy on bearing capacity of a footing. Humpheson and Lewis (1975), Perkins and Madson (2000) proposed an approach to predict accurately bearing capacity of shallow foundations on sand through introducing relative dilatancy index. However, those studies of bearing capacity and strain based on classical continuum theories don't take account into the following factors such as strain softening, particle size and the stress-level. Because classical continuum theories have no internal length scale, they can't be used to model the particle size effect on behavior of granular materials. In addition, the presence of strain softening brings that the initial and boundary value problem will become ill-posed after the onset of localization, which results in pathologically mesh-dependent solutions of numerical analysis of finite element method. Some types of regularization mechanism or non classical continuum model such as Cosserat or micro-polar continuum theory may be used to overcome the mesh-dependent in softening problem (Manzari and Yonten 2011). Cosserat continuum theory has the rotational degree of freedom and internal length scale (de Borst 1991, Li and Tang 2005).

This work is based on the work of Li and Tang (2005), a non-associated flow rule with evolution of dilation angle is used to consider the influence of dilatancy. Numerical examples focus on the bearing capacity and localization of granular assemblies. Results shows that the evolution of dilatancy has different tendency in shear band, and the dilatancy has different effect on bearing load and strain localization for different problems. Results illustrate the capability and performance of the presented model in modeling the effect of dilatancy on failure behavior of granular materials.

2. The dilatancy and the plastic potential function

2.1 The dilatancy of granular materials

Many features of granular materials, such as the reduction of friction angle with increasing stress level, are related to dilatancy. Therefore, the understanding of dilatancy is the key to the understanding of behavior of granular materials. The link between the friction angle and dilatancy, and the link between the dilation angle and the density and pressure are central topics of behavior of granular materials (Houlsby 1991). The dilation angle is usually defined by the following equation

$$\sin\psi = \frac{d\varepsilon_v^p}{d\varepsilon_s^p} = \frac{d\varepsilon_1^p + d\varepsilon_2^p + d\varepsilon_3^p}{d\varepsilon_1^p - d\varepsilon_3^p} \tag{1}$$

In which, ψ is the dilation angle, $d\varepsilon_v^p$ and $d\varepsilon_s^p$ are the plastic volumetric strain and the plastic shear strain, respectively, $d\varepsilon_i^p$ $(i = 1, 2, 3)$ are the principal strain increments. Equation one shows

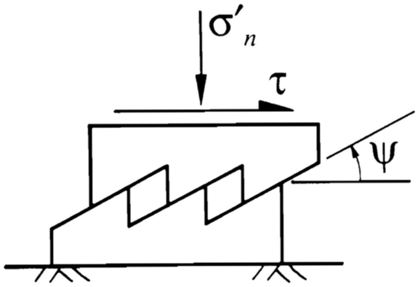

Fig. 1 The sawtooth model

that the dilation angle is strictly defined in terms of the plastic components of strain increments, not the total strain increments. However, the plastic strain increments are often instead of the total strain increment because the elastic strain are much smaller than the plastic strains in practice.

The relationship between the friction and dilation angle is often interpreted by the sawtooth model, shown in Fig. 1. It can be seen that there is a sliding on a rough plane represented by a sawtooth with teeth at angle ψ to the horizontal, and the plane is with the friction angle φ_{cv} acting on the teeth. The relationship between the observed shear and normal stress can be derived as the following when sliding occurs

$$\frac{\tau}{\sigma_n} = \tan\varphi = \tan(\varphi_{cv} + \psi) \tag{2}$$

In which φ is the apparent friction angle, φ_{cv} is the friction angle at constant volume. The equation two implies that $\varphi = \varphi_{cv} + \psi$, which give the relationship between the friction and dilation angle. Many theories have been put forward to explain this relationship (Taylor 1948, Schofield and Wroth 1968, Rowe 1962, Bolton 1986, Houlsby 1991). However, the evolution of dilation angle is not very clear for most engineers. The dilatancy generally is considered in engineering analysis by the following approaches:

(1) With associated flow rule, assuming that the material dilation angle ψ is equal to its internal friction angle φ;
(2) With $\psi = 0°$ in the non-associated flow rule;
(3) With ψ is a constant within the range of $0° \sim \varphi$ in non-associated flow rule.

These approaches all have some drawbacks. The first expands the dilatancy of geomaterials and it is against the plastic energy dissipation theory. The second doesn't consider dilatancy entirely, it obviously conflicts with the properties of the most of geotechnical materials. The last is better than the previous manners so it is applied in most cases. However the last is also a way of over-reliance on engineering experience, there is not a strict criterion to give the specific value. In addition, the last means dilatancy increases with the shear strain increasing linearly because the dilation angle is kept as a constant. However this isn't consistent with the phenomena that the plastic volume doesn't increase in the critical state. Therefore, the evolution of dilatancy should be considered in modeling of behavior of granular materials. In this paper, the expression of dilation angle suggested by Houlsby is adopted to consider its evolution with density and pressure, which combine the Wroth's critical state line function with Bolton's empirical fit, presented as the following

$$\psi = -0.11 + 0.59 I_D - 0.11 I_D \ln\left(\frac{p'}{p_a}\right) \tag{3}$$

Where p_a is a standard atmospheric pressure, p' is the current hydrostatic stress, $I_D = \dfrac{e_{\max} - e}{e_{\max} - e_{\min}}$, is the relative density, the maximum and minimum void ratios $e_{\max}$ and $e_{\min}$ are obtained from standard tests, e is the current void ratio. It is well known that the main deformation mechanism of granular materials is the particles rearrangement owing to that relative motion between the particles without considering particle breakage. Further assuming the deformation of particles themselves can be ignored, and then evolution of the current void ratio can be expressed as $\dot{e} = (1+e) tr\varepsilon$.

2.2 The plastic potential function and Cosserat model

Cosserat theory and its numerical method have been presented by few researchers (Li and Tang 2005, de Borst 1991). In their woks Drucker-Prager yield criterion has been used to compute the plastic strain, viz.

$$F = q + A_{\varphi} p + B = 0 \tag{4}$$

Where

$$A_{\varphi} = \frac{6 \sin\varphi}{(3 + \sin\varphi)}; \qquad B = \frac{-6c \sin\varphi}{(3 + \sin\varphi)} \tag{5}$$

In which φ and c are internal friction angle and cohesion, respectively. The effective deviatoric stress q and the hydrostatic stress p can be written as

$$q = \left(\frac{1}{6}\boldsymbol{\sigma}^{\mathrm{T}} \mathbf{P} \boldsymbol{\sigma}\right)^{1/2}, \quad p = \frac{1}{3}(\sigma_{xx} + \sigma_{yy} + \sigma_{zz}) \tag{6}$$

Where

$$\mathbf{P} = \begin{bmatrix} 2 & -1 & -1 & & & & \\ -1 & 2 & -1 & & & & \\ -1 & -1 & 2 & & & & \\ & & & 3/2 & 3/2 & & \\ & & & 3/2 & 3/2 & & \\ & & & & & 3 & \\ & & & & & & 3 \end{bmatrix}$$

The stress and strain vector in the two dimensional Cosserat model can be defined as

$$\boldsymbol{\sigma} = [\sigma_{xx} \;\; \sigma_{yy} \;\; \sigma_{zz} \;\; \sigma_{xy} \;\; \sigma_{yx} \;\; m_{zx}/l_c \;\; m_{zy}/l_c]^{\mathrm{T}} \tag{7a}$$

$$\boldsymbol{\varepsilon} = [\varepsilon_{xx} \;\; \varepsilon_{yy} \;\; \varepsilon_{zz} \;\; \varepsilon_{xy} \;\; \varepsilon_{yx} \;\; \kappa_{zx}/l_c \;\; \kappa_{zy}/l_c]^{\mathrm{T}} \tag{7b}$$

It will leads to the following equations based on the additive decomposition of strain and generalized Hooke's

$$\boldsymbol{\sigma} = \mathbf{D_e}\boldsymbol{\varepsilon}_\mathbf{e}; \qquad \boldsymbol{\varepsilon}_\mathbf{e} = \boldsymbol{\varepsilon} - \boldsymbol{\varepsilon}_\mathbf{p} \tag{7c}$$

Where κ_{zx} and κ_{zy} are the micro-curvatures in Cosserat model, m_{zx} and m_{zy} are the couple stresses conjugated to κ_{zx} and κ_{zy}, respectively. l_c is the internal length scale, ε_e and ε_p are the elastic and plastic parts of strain, the notion

$$\mathbf{D_e} = \begin{bmatrix} \lambda+2G & \lambda & \lambda & & & & \\ \lambda & \lambda+2G & \lambda & & & & \\ \lambda & \lambda & \lambda+2G & & & & \\ & & & G+G_c & G-G_c & & \\ & & & G-G_c & G+G_c & & \\ & & & & & 2G & \\ & & & & & & 2G \end{bmatrix}$$

is elastic modulus matrix for isotropic materials. λ and G are lame constants, G_c is Cosserat shear modulus.

A plastic potential function is introduced into classical elastoplastic theory for calculating the plastic strain increment. The plastic potential function is taken in the following form, which corresponds to Drucker-Prager yield

$$G = q + A_\psi p + B \tag{8}$$

Where

$$A_\psi = \frac{6\sin\psi}{(3+\sin\psi)} \tag{9}$$

In which ψ is the dilation angle, in this study, the equation three is used to account its evolution with density and hydrostatic stress.

3. Numerical examples

The numerical examples focus on square panel in the plane strain and the slope problem.

3.1 Square panel

The first example concerns a homogeneous square panel with side length 20 m (Li and Tang 2006), which is subjected to uniaxial compression between two rigid plates controlled by the vertical displacement as shown in Fig. 2. The horizontal displacements of finite element nodes which are on the top and bottom boundary are fixed as zero. we just consider 10 m × 10 m square as computational domain owing to the symmetry condition. Material parameters are as follows: $E = 5.0 \times 10^7$ N/m^2, $\upsilon = 0.3$, $G_C = 1.0 \times 10^7$ N/m^2, $l_c = 0.15$ m, $c_0 = 1.5 \times 10^5$ N/m^2, $h_p = -1.5 \times 10^5$ N/m^2, $\varphi = 37°$, $e_{\max} = 0.84$, $e_{\min} = 0.41$. The specific vertical displacement on the top is 0.2 m, and

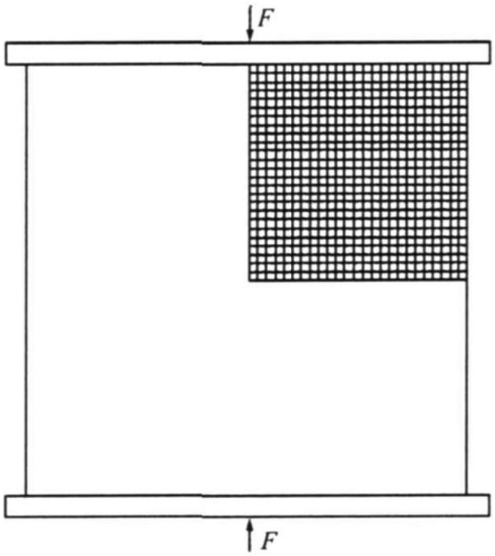

Fig. 2 The square panel in plane strain

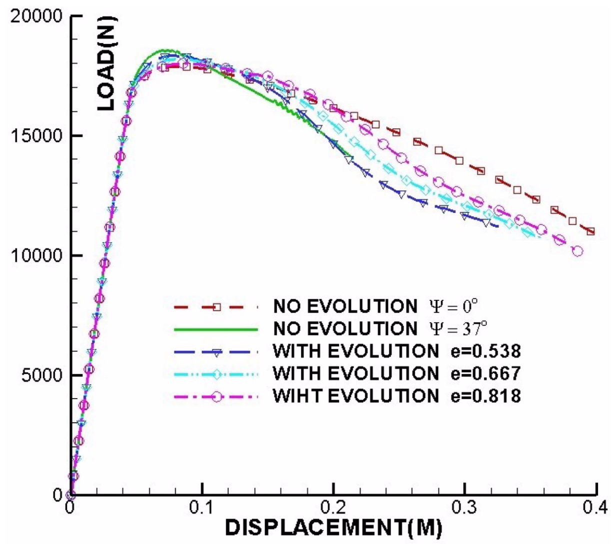

Fig. 3 Curves of the vertical load applied to the top of the square panel with increasing prescribed vertical displacement of top surface

three different initial porosities, $n = 0.35$, 0.4, 0.45, are given for considering the effects of density. The curves of the vertical load applied to the top of the square panel with increasing prescribed vertical displacement of the top surface are shown in the Fig. 3. It is seen that the difference of capacity is small whether dilatancy evolution are adopted or not. However, when the evolution of dilation angle is considered, bearing capacity decreases with increase of the initial porosity, but the residual values increase with the initial porosity after the peak of the bearing capacity. Moreover,

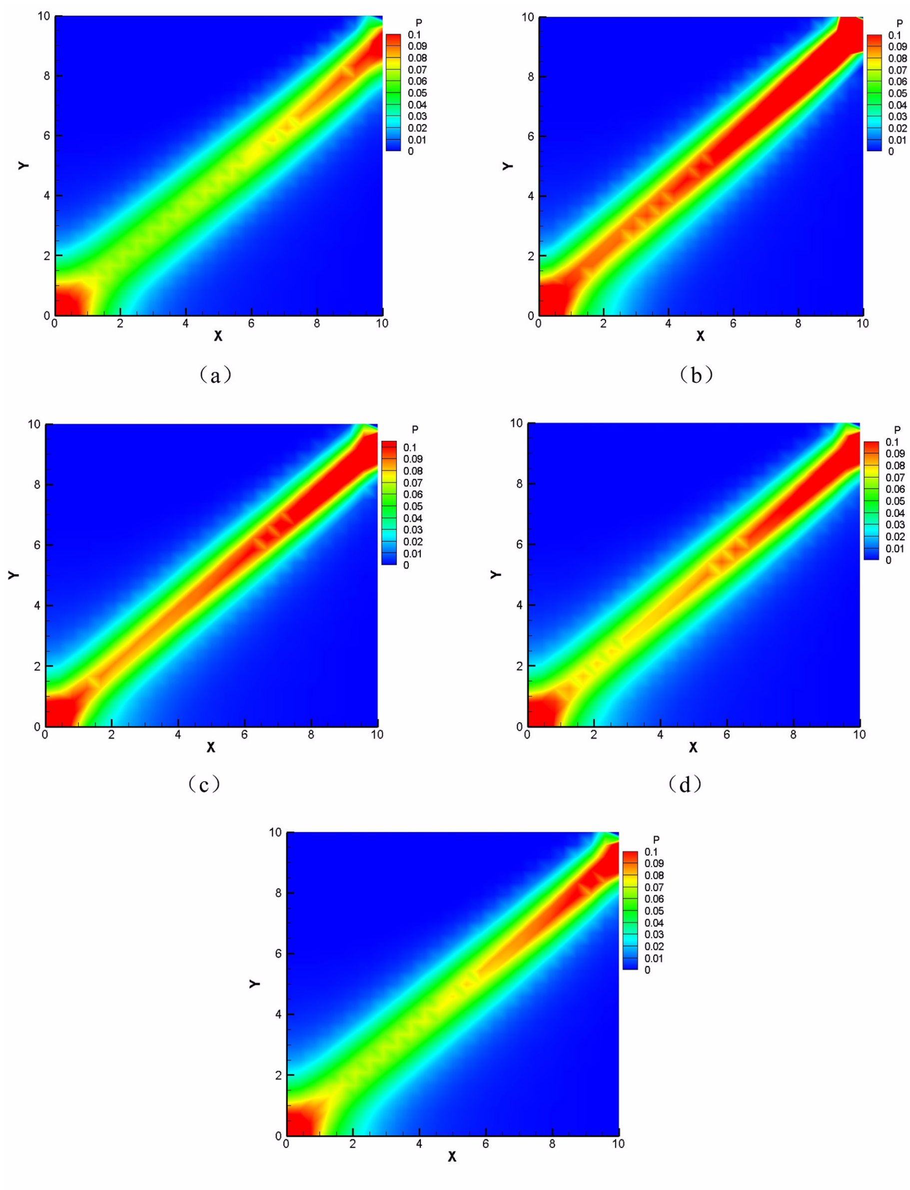

Fig. 4 Effective plastic strain distribution in the square panel subjected to a prescribed vertical displacement 1 m at the top of the panel: (a) without evolution of dilation angle, PSAI = 0º, (b) without evolution of dilation angle, PSAI = 37º, (c) with evolution of dilation angle, $e = 0.538$, (d) with evolution of dilation angle, $e = 0.667$ and (e) with evolution of dilation angle, $e = 0.818$

the introduction of evolution of dilation angle causes the slight nonlinear behavior after the peak. Effective plastic strain distributions in the panel subjected to a prescribed vertical displacement 1 m are shown in Fig. 4, it is seen that the width of shear band given by different methods are also similar. However, the intensity of plastic strain is distinct. The minimum value corresponds to

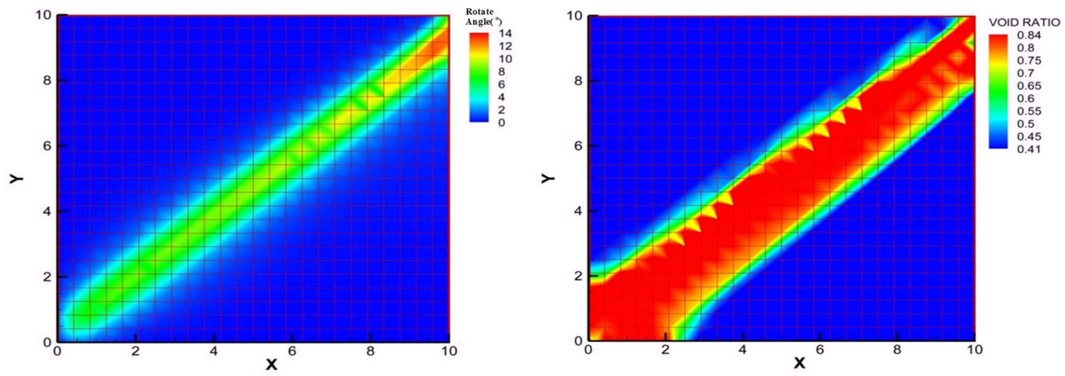

Fig. 5 Distribution of the porosity and rotation angle in the square panel subjected to a prescribed vertical displacement 1 m at the top of the panel: (a) rotation angle and (b) porosity

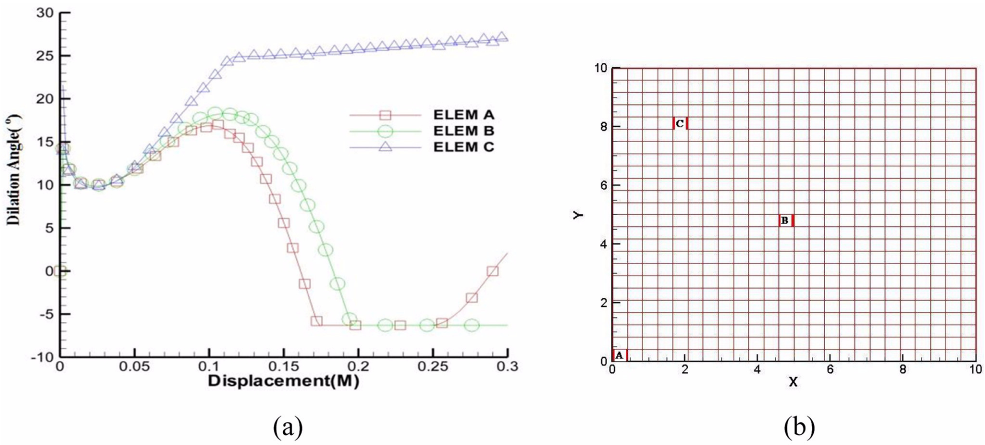

Fig. 6 The evolution of the dilatancy: (a) the curves and (b) the location of elements

$\psi = 0^o$ while the maximum corresponds to $\psi = 37^o$. The middle intensity of plastic strain corresponds to the evolutionary dilation angle, and that increases with decreasing of the initial porosity.

One of advantages of the present model is that it can consider the evolution of the porosity and the rotation angle in granular assemblies. The distribution of the porosity and rotation angle in the panel subjected to a prescribed vertical displacement 1 m are shown in Fig. 5. It can be seen there are the higher porosity and the larger rotation degree in shear band. These agree with the experiment and numerical results by discrete element method (Iwashita and Oda 1998, Li *et al.* 2005).

However, the evolution of dilatancy based on the Eq. (3) and Drucker-Prager yield criterion is different from the critical state theory. The evolution of dilatancy of different location are shown in Fig. 6, it can be seen that the dilatancy inside or outside the shear band does not tends to vanish after the peak of the strength.

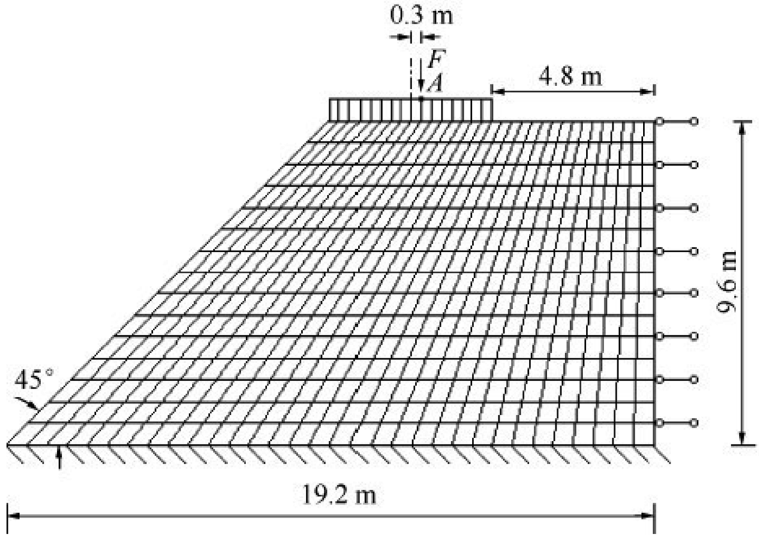

Fig. 7 The slope: boundary condition and mesh of FEM

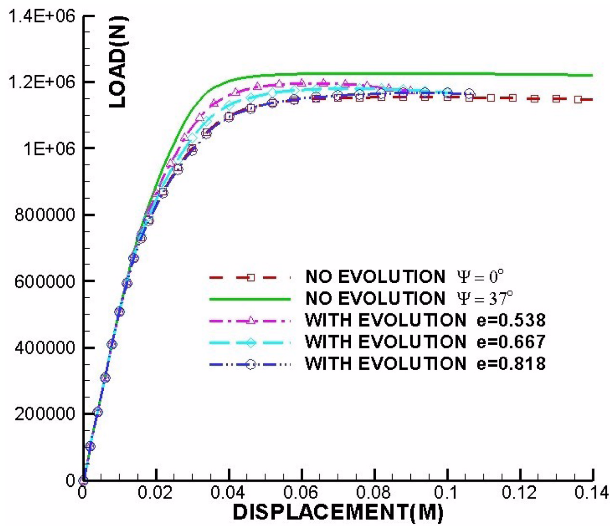

Fig. 8 Curves of the vertical load with increasing prescribed vertical displacement

3.2 Slope stability

This example considers the problem of slope stability. The force exerted by the foundation placed on the top of slope by prescribed displacement as shown in Fig. 7. The contact surface between slope and foundation is assumed to be ideal bond. Material parameters are as follows: $E = 5.0 \times 10^7$ N /m^2, $\upsilon = 0.3$, $c_0 = 5.0 \times 10^4$ N/m^2, $h_p = -3.0 \times 10^4$ N/m^2, φ=37°, $G_C = 1.0 \times 10^7$ N/m^2, $l_C = 0.12$, $e_{\max} = 0.84$, $e_{\min} = 0.41$, the initial porosities are same as the previous example. The load-displacement curves are shown in the Fig. 8, it is seen that the bearing capacity is obvious different

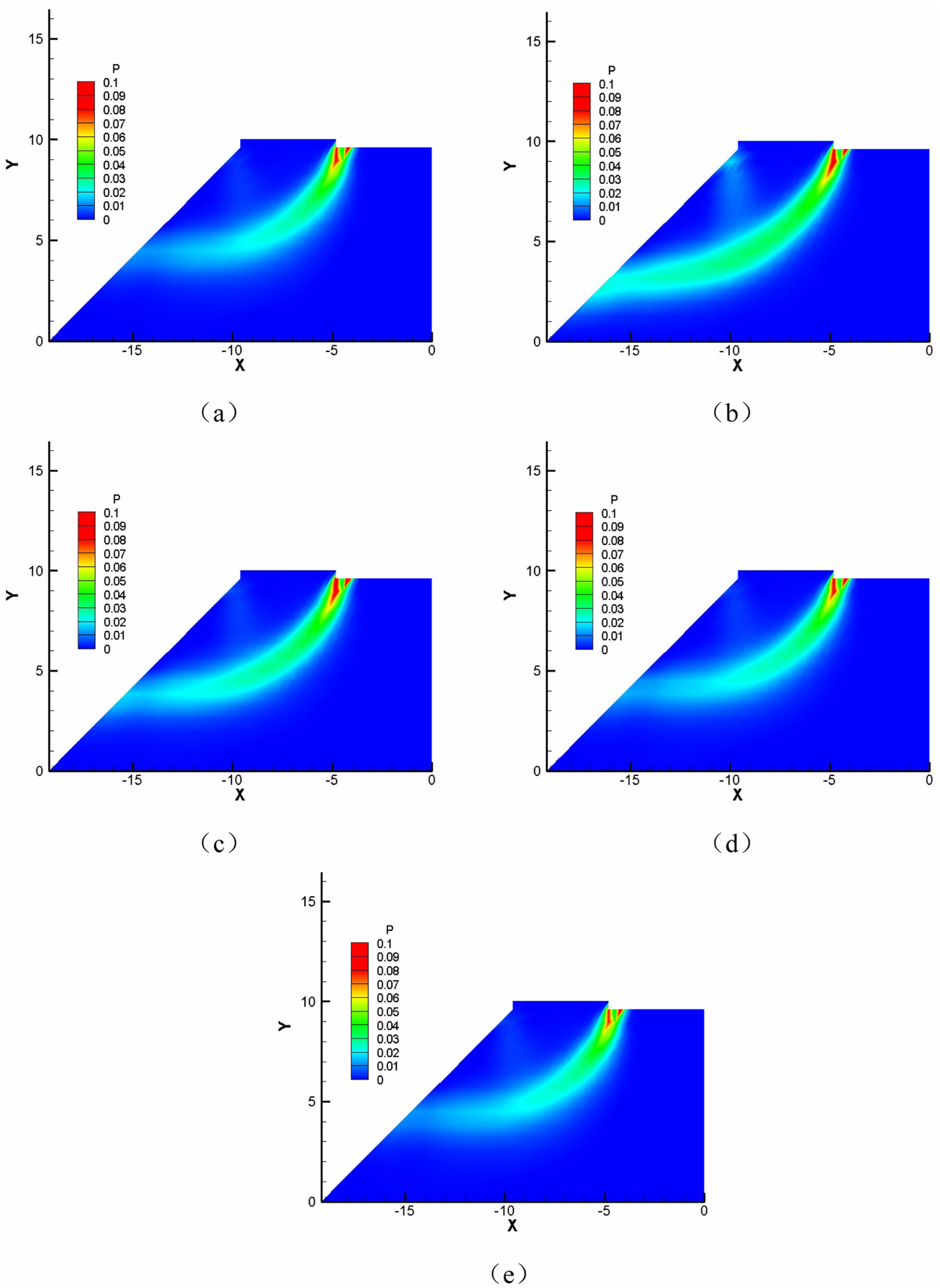

Fig. 9 Effective plastic strain distribution in the slope subjected to a prescribed vertical displacement 4 m: (a) without evolution of dilation angle, $\psi = 0$, (b) without evolution of dilation angle, $\psi = 37^{o}$, (c) with evolution of dilation angle, $e = 0.538$, (d) with evolution of dilation angle, $e = 0.667$ and (e) with evolution of dilation angle, $e = 0.818$

according to different method to deal with dilation angle. The maximum bearing capacity corresponds to associated flow, i.e., $\psi = 37^{o}$ while the minimum corresponds to $\psi = 0^{o}$, and the

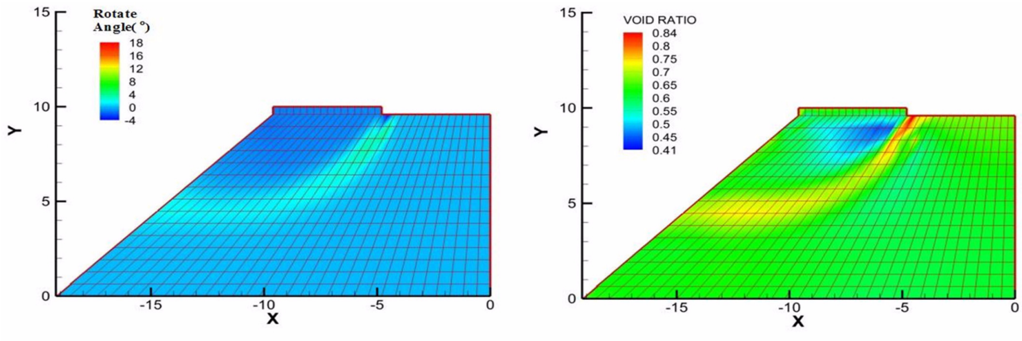

(a) (b)

Fig. 10 Distribution of the porosity and rotation angle in the slope subjected to a prescribed vertical displacement 4 m: (a) rotation angle and (b) porosity

middle bearing capacity corresponds to the evolutionary dilation angle. And the bearing capacity increases with decreasing of the initial porosity when accounting the evolution of the dilation angle. Effective plastic strain distributions in the slope subjected to a prescribed vertical displacement 1 m are shown in the Fig. 9, it can be seen that there are some difference in localization patterns. The shear band obviously run through the slope and corresponds to a deeper slip if the value of dilation angle being taken as 37^{o}, however, the shear band doesn't run through the slope when $\psi = 0$. If the evolution of the dilation angle is introduced, the depth of slip increases gradually with decreasing of the initial porosity and the shear band more trends to run through. The distributions of the porosity and rotation angle are shown in the Fig. 10. It can be seen that there are the higher porosity and the larger rotation degree in shear band.

4. Conclusions

The evolution of the dilation angle with density and stress state is discussed, and the specify formula given by Houlsby is introduced into the elastoplasticity theory of Cosserat model for granular materials. The numerical examples show that the evolution of dilation angle has, to some extent, effect on bearing capacity and strain localization. However, the degree of influence is different in each case. For slope stability problem, the prediction of the depth of slip will be different if adopting the different method of dealing with the dilation angle, and the bearing capacity increase with the value of dilation angle.

Acknowledgements

The authors are pleased to acknowledge the support of this work by the National Natural Science Foundation of China through contract/grant number 10802060 and 11172216 and the Natural Key Basic Research and Development Program of China (973 Program) through contract/grant numbers 2010CB731502. And the first author would like to express his hearty thanks professor Tang hongxiang of Dalian University of Technology, for his kind help.

References

Alsaleh, M., Kitsabunnarat, A. and Helwany, S. (2009), "Strain localization and failure load predictions of geosynthetic reinforced soil structures", *Interact. Multiscale Mech.*, **2**(3), 235-261.

Aristoff, D. and Radin, C. (2011), "Dilatancy transition in a granular model", *J Stat. Phys*., **143**(2), 215-225.

Bolton, M.D. (1986), "The strength and dilatancy of sands", *Geotechnique*, **36**(1), 65-78.

De Borst, R. (1991), "Simulation of strain localization: a reappraisal of the Cosserat continuum", *Eng. Computation*., **8**(4), 317-332.

Desimone, A. and Tamagnini, C. (2005), "Stress-dilatancy based modelling of granular materials and extensions to soils with crushable grains", *Int. J. Numer. Anal. Mech. Geomech*., **29**(1), 73-101.

Guo, P.J. and Su, X.B. (2007), "Shear strength, interparticle locking, and dilatancy of granular materials", *Can. Geotech. J*., **44**(5), 579-591.

Houlsby, G.T. (1991), *How the dilatancy of soil affects their behavior*, The written version of an invited lecture delivered at the tenth European conference on soil mechanics and foundation engineering, Florence, Italy.

Iwashita, K. and Oda, M. (1998), "Rolling resistance at contacts in simulation of shear band development by DEM", *J. Eng. Mech*., **124**(3), 285-292.

Li, X.K., Chu, X.H. and Feng, Y.T. (2005), "A discrete particle model and numerical modeling of the failure modes of granular materials", *Eng. Computation*., **22**(8), 894-920.

Li, X.K. and Tang, H.X. (2005), "A consistent return mapping algorithm for pressure-dependent elastoplastic Cosserat continua and modeling of strain localization", *Comput. Struct*., **83**(1), 1-10.

Manzari, M.T and Yonten, K. (2011), "Analysis of post-failure response of sands using a critical state micropolar plasticity model", *Interact. Multiscale Mech.*, **4**(3), 187-206.

Massoudi, M. and Mehrabadi, M.M. (2001), "A continuum model for granular materials: considering dilatancy and the Mohr-Coulomb criterion", *Acta Mech*., **152**(1-4), 121-138.

Perkins, S.W. and Madson, C.R. (2000), "Bearing capacity of shallow foundations on sand: a relative density approach", *J. Geotech. Geoenviron. Eng*., **126**(6), 521-530.

Rowe, P.W. (1962), "The stress-dilatancy relation for static equilibrium of an assembly of particles in contact", *Proc. of Royal. Soc.* A, **269**(1339), 500-527.

Ueng, T.S. and Chen, T.J. (2000), "Energy aspects of particle breakage in drained shear of sands", *Geotechnique*, **50**(1), 65-72.

Wan, R.G. and Guo, P.J. (1999), "A pressure and density dependent dilatancy model for granular materials", *Soils Found*., **39**(6), 1-11.

Zhang, J. and Salgado, R. (2010), "Stress-dilatancy relation for Mohr-Coulomb soils following a non-associated flow rule", *Geotechnique*, **60**(3), 223-226.